

---

Article

# Nanocellulose production using ionic liquids with enzymatic pretreatment

Marta Babicka <sup>1</sup>, Magdalena Woźniak <sup>1</sup>, Kinga Szentner <sup>1</sup>, Monika Bartkowiak <sup>2</sup>, Barbara Peplińska <sup>3</sup>, Krzysztof Dwiecki <sup>4</sup>, Sławomir Borysiak <sup>5</sup> and Izabela Ratajczak <sup>1,\*</sup>

<sup>1</sup> Department of Chemistry, Faculty of Forestry and Wood Technology, Poznań University of Life Sciences, Wojska Polskiego 75, 60625 Poznań, Poland

<sup>2</sup> Department of Chemical Wood Technology, Faculty of Forestry and Wood Technology, Poznań University of Life Sciences, Wojska Polskiego 38/42, 60627 Poznań, Poland

<sup>3</sup> NanoBioMedical Centre, Adam Mickiewicz University, Wszechnicy Piastowskiej 3, 61-614 Poznań, Poland

<sup>4</sup> Department of Food Biochemistry and Analysis, Poznań University of Life Sciences, Mazowiecka 48, 60-623 Poznań, Poland

<sup>5</sup> Institute of Chemical Technology and Engineering, Poznan University of Technology, Berdychowo 4, 60965 Poznań, Poland

\* Correspondence: izabela.ratajczak@up.poznan.pl

**Abstract:** Nanocellulose has gained increasing attention during the past decade, which is related to its unique properties and wide application. In this paper, nanocellulose was produced by hydrolysis with ionic liquids (1-ethyl-3-methylimidazole acetate (EmimOAc) and 1-allyl-3-methylimidazolium chloride (AmimCl)) from microcrystalline cellulose (Avicel and Whatman) subjected to enzymatic pretreatment. The obtained material was characterized by Fourier transform infrared spectroscopy (FTIR), X-ray diffraction (XRD), dynamic light scattering (DLS), scanning electron microscope (SEM) and thermogravimetric analysis (TG). The results showed that the nanocellulose had a regular and spherical structure with a diameter of 30-40 nm and exhibited lower crystallinity and thermal stability than the material after hydrolysis with *Trichoderma reesei* enzymes. However, the enzyme-pretreated Avicel had a particle size of about 200 nm and a cellulose II structure. A two-step process involving enzyme-pretreatment and hydrolysis with ionic liquids resulted in the production of nanocellulose. Moreover, the particle size of nanocellulose and its structure depend on the ionic liquid used.

**Keywords:** nanocellulose; ionic liquids; *Trichoderma reesei*; enzymatic hydrolysis

---

## 1. Introduction

Nanocellulose has gained increasing attention during the past decade, which is confirmed by the number of patents and scientific papers concerning its properties, production methods and potential applications [1,2]. Cellulose nanocrystals have found applications in various fields in our life, such as food packaging, biodegradable polymers, biomedical utilization (including drug delivery, substituted implants, biocatalyst or tissue regeneration), wood adhesives or use as a filler or additive to nanocomposites [2–10]. Nanocellulose-based polymer composites have potential applications as adsorptive, filtering and decontaminating materials (including water treatment, air purification or microbe and viral decontamination), as well as materials in binders, separators and electrodes of energy conservation devices and energy capture devices e.g. as CO<sub>2</sub> separators [8,11–15]. The wide application of nanocellulose is connected with its unique properties, such as high surface area, light weight, low density, biodegradability, biocompatibility and outstanding strength properties [16–18].

Numerous methods to produce cellulose with nanometric dimensions from different lignocellulose materials, including mechanical (e.g. grinding, grating), chemical (e.g. with the use of acids and bases) and physical methods (e.g. with the use of high-power lasers) are applied [19–21]. A common method of nanocellulose production is acid hydrolysis and its modifications, where sulfuric, hydrobromic and hydrochloric acids are usually used in the process of cellulose hydrolysis [8,22,23]. However, acid hydrolysis is not considered an environmentally-friendly method due to the use of large amounts of solvents, which generates a considerable volume of sewage that requires treatment and contributes to the corrosion of reactors. Moreover, acid hydrolysis characterized by the low efficiency of nanocellulose production, formation of cellulose nanocrystals with reduced thermal stability [24–26].

An eco-friendly alternative method of nanocellulose production is the application of ionic liquids or enzymes, since these methods do not generate hazardous waste, as is the case with acid hydrolysis. Different classes of enzymes have been applied in nanocellulose preparations, including cellulases, xylanases and lytic polysaccharide monooxygenases [27]. However, cellulases, which are produced by cellulolytic organisms, including fungal species such as *Aspergillus*, *Trichoderma* or *Clostridium*, are the most common in preparation of nanocellulose [27,28]. It is generally recognized that complete hydrolysis of cellulose to glucose requires a synergistic action of at least two of the three groups, into which cellulases are divided: endoglucanases, exoglucanases and cellobiohydrolases [1,29]. However, for the production of nanocellulose, endoglucanases are of greatest interest due to their action mainly on amorphous cellulose [30]. It should also be emphasized that the efficiency of the enzymatic hydrolysis process depends on the types of cellulolytic enzymes that determine the size of nanometric particles, as well as their polydispersion [28]. According to literature data, enzymes are used in the extraction of nanometric cellulose, both alone or combined with chemical or mechanical methods [22,27,31–38]. Moreover, the efficiency of cellulose enzymatic hydrolysis processes depends on the cellulose polymorphs [39].

Ionic liquids, often referred to as green solvents, have also been used in the production of nanocellulose [40–43]. Ionic liquids (ILs) are generally defined as salts that melt below 100 °C and are completely composed of ions. Interestingly, ILs have many attractive properties such as chemical and thermal stability, low melting point, non-volatility and non-flammability, low vapor pressure and recyclability [44,45]. Various types of ionic liquids are used in nanocellulose hydrolysis, including 1-butyl-3-methylimidazolium hydrogen sulfate, 1-butyl-3-methylimidazolium chloride and 1-ethyl-3-methylimidazole chloride [23,46–51]. Production of nanocellulose by means of ionic liquids has such benefits as e.g. the potential to use atmospheric pressure, small amounts of solvents, the potential for regeneration of ionic liquids, working with an odorless and relatively safe solvent or generation of relatively smaller amounts of sewage. On the other hand, this method has also disadvantages, which include the relatively high cost of ionic liquids or the unsatisfactory efficiency of the extraction process [49,52–57].

A combination of methods has been used to increase the efficiency of the nanocellulose production process. The aim of pretreatment is to bring the cellulose polymers to an appropriate form that will increase the efficiency of the subsequent process of nanocellulose production itself. Pretreatment can be a physical or chemical process, most often it is associated with reducing the particle size of cellulose, increasing its porosity and surface area, or reducing crystallinity [58,59]. The production of nanocellulose by enzymatic hydrolysis was preceded by various methods of initial preparation of the starting material, including mechanical and chemical methods [1,27,60]. Prior to the enzymatic hydrolysis reactions, the lignocellulosic material was pretreated by milling, swelling treatment, steam explosion, sonification or treatment with a sodium hydroxide aqueous solution [22,31,37,61,62]. Ionic liquids (e.g. 1-butyl-3-methylimidazolium chloride, 1-ethyl-3-methylimidazolium acetate and 1-allyl-3-methylimidazolium chloride) were also applied as pretreating agents in enzymatic

hydrolysis [63–66]. The pretreated cellulosic materials had an increased surface area promoting the effective action of enzymes, increased absorption of cellulases and improving efficiency of the whole process [63–66].

In our paper, we used enzymatic hydrolysis of cellulosic materials as a preliminary stage of nanocellulose preparation with the application of ionic liquids. To our best knowledge, this is the first time that enzymatic hydrolysis has been combined with treatment with ionic liquids to obtain nanocellulose, where enzymatic hydrolysis is the pretreatment step. Therefore, the aim of the study was to produce nanometric cellulose by pretreatment with the cellulolytic enzyme from *Trichoderma reesei*, followed by treatment with two ionic liquids: 1-ethyl-3-methylimidazole acetate (EmimOAc) and 1-allyl-3-methylimidazolium chloride (AmimCl). The obtained material was characterized by Fourier transform infrared spectroscopy (FTIR), X-ray diffraction (XRD), dynamic light scattering (DLS), thermogravimetric analysis (TG) and scanning electron microscope (SEM).

## 2. Materials and Methods

### 2.1. Materials

Microcrystalline cellulose: Avicel PH-101 and Whatman cellulose filter paper No. 1 were purchased from Sigma Aldrich Chemie GmbH (Darmstadt, Germany). The cellulolytic enzyme from a microscopic fungus *Trichoderma reesei* ATCC 26921 with the activity of 700 units/g and ionic liquids: 1-allyl-3-methylimidazolium chloride ( $\geq 97.0\%$ ) and 1-ethyl-3-methylimidazolium acetate ( $\geq 95.0\%$ ) were also purchased from Sigma Aldrich Chemie GmbH (Darmstadt, Germany).

### 2.2. Pretreatment of Cellulose with Cellulolytic Enzyme

The cellulose material (Avicel and Whatman) was added to a citrate buffer (50 mM, pH = 4.8) at a ratio of 50 : 1 (mg/mL) and was incubated for 30 min at 50 °C with a shaking speed of 150 rpm/min (Incubated Shaker, Lab Companion, JeioTech, Korea). Afterwards the cellulolytic enzyme diluted in the enzymatic citrate buffer (1:50 by volume) was added to the cellulose material at a ratio of 1:2 by volume. The mixture was incubated at 50 °C with a shaking speed of 150 rpm for 30 min. The reaction was stopped by boiling the sample for 5 minutes. Next, the samples were centrifuged at 1000 rpm/min for 15 minutes and washed by deionized water. The solid cellulose residue was dried (Pol-Eko-Aparatura, Wodzisław Śląski, Poland) and used for further analysis.

### 2.3. Preparation of Cellulose Nanocrystals by Ionic Liquids

The cellulose material (Avicel and Whatman) after pretreatment with the *Trichoderma reesei* enzyme was mixed with ionic liquids ([EmimOAc] and [AmimCl]) at a ratio of 1:5 by weight. The reactions were run until the material had dissolved (~15 min) at 80 °C, under intense stirring using a heating mantle with magnetic stirring (ChemLand, Stargard, Poland). The reaction was carried out without solvent. The reaction was stopped by adding 15 mL of an acetone and water mixture (1:1) to the reaction mixture. The products of reactions were washed with the acetone and water mixture, filtered, and dried initially at room temperature and finally over P<sub>2</sub>O<sub>5</sub> (Sigma Aldrich Chemie GmbH, Darmstadt, Germany).

### 2.4. Methods

#### 2.4.1 FTIR Spectroscopy

Fourier transform infrared spectroscopy was used to characterize the obtained materials and determine their chemical structure. All samples (1 mg) were mixed with KBr (200 mg) (Sigma Aldrich Chemie GmbH, Darmstadt, Germany) and analyzed in the pastille form. Spectra were recorded in the range from 4000 to 500 cm<sup>-1</sup>, resolution 2 cm<sup>-1</sup>

and 16 scans were recorded on a Nicolet iS5 spectrophotometer (Thermo Fisher Scientific, Waltham, MA, USA).

#### 2.4.2. XRD Analysis

The supermolecular structure of cellulose samples after enzymatic hydrolysis and enzyme-pretreatment cellulose treated with ionic liquids was analyzed by X-ray diffraction (XRD). The samples were determined using a TUR M-62 X-ray diffractometer (Carl Zeiss AG, Jena, Germany) with a copper anode. The wavelength of the Cu  $K_{\alpha}$  radiation source was 1.5418 Å, and the spectra were obtained at 30 mA with an accelerating voltage of 40 kV. The diffraction pattern was recorded between 5 and 30° (2 $\theta$ -angle range) in the step of 0.04°/3 s. Deconvolution of peaks was performed by the method proposed by Hindeleh and Johnson [67] and improved and programmed by Rabiej [68]. After separation of XRD lines, the degree of crystallinity ( $X_c$ ) of cellulose samples by comparing areas under crystalline peaks and the amorphous curve was determined.

#### 2.4.3. DLS Analysis

The particle size (hydrodynamic diameter) of cellulose samples was determined by the DLS method using a Zetasizer Nano ZS-90 (Malvern Instruments Ltd., Malvern, UK). Before analysis, the tested materials were mixed (2 mg) with deionized water (5 mL) and treated using an ultrasound system (Sonic-2; Polsonic Palczyński Sp. J., Warsaw, Poland) for 25 min.

#### 2.4.4. SEM Analysis

The surface morphology of micro- and nanocrystalline cellulose was examined by the SEM method. Images were taken with the use of a JEOL JSM-7001F TTLS scanning electron microscope (JEOL Ltd., Tokyo, Japan) applying the accelerating voltage of 5 kV and a secondary electron (SEI) detector. The samples were placed on a carbon tape and investigated without coating.

#### 2.4.5. TG Analysis

Thermogravimetric analysis was performed on the Netzsch STA 449 F5 Jupiter apparatus (Erich NETZSCH GmbH & Co. Holding KG, Selb, Germany). The samples (15  $\pm$  1 mg) were heated to 600 °C at a rate of 10 °C/min. The analyses were performed in an atmosphere of helium flowing through the furnace space at a rate of 15 mL/min. Thermogravimetric curves (TG) and differential thermogravimetric curves (DTG) were recorded on the thermograms. The former illustrate the dependence of the change in mass (mass loss) on temperature, the latter the rate of this change.

### 3. Results and Discussion

#### 3.1. FTIR Analysis

In the first stage of the research, the chemical structure of the cellulose samples was determined using Fourier transform infrared spectroscopy (FTIR). The FTIR spectra of the cellulose material after enzymatic hydrolysis and the material obtained after the two-step nanocellulose production process (pretreatment with the enzyme and treatment with ionic liquids) are shown in Figures 1 and 2.

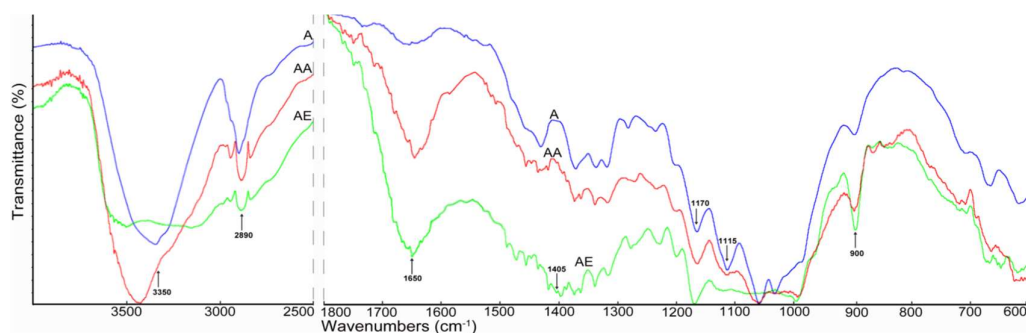


**Figure 1.** FTIR spectra of (A) enzyme-pretreated Avicel cellulose; (AA) enzyme-pretreated Avicel cellulose treated with AmimCl; (AE) enzyme-pretreated Avicel cellulose treated with EmimOAc.

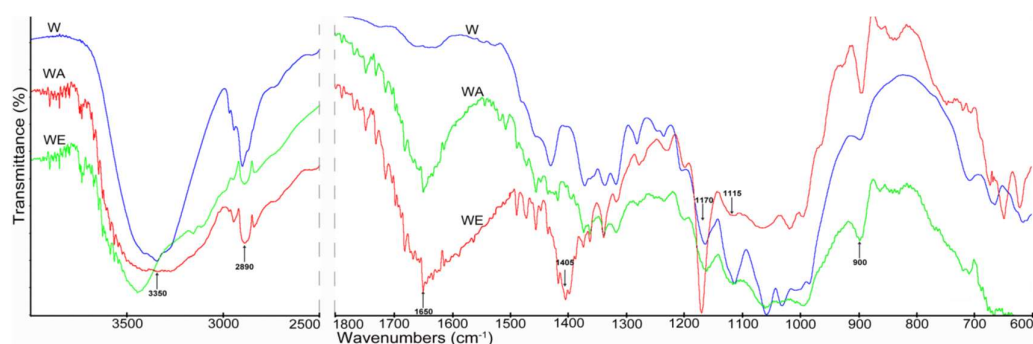


**Figure 2.** FTIR spectra of (W) enzyme-pretreated Whatman cellulose; (WA) enzyme-pretreated Whatman cellulose treated with AmimCl; (WE) enzyme-pretreated Whatman cellulose treated with EmimOAc.

All cellulose samples (Avicel and Whatman), both after enzyme hydrolysis and enzyme-pretreated cellulose hydrolyzed with ionic liquids, present a broad band in the region of 3350-3480  $\text{cm}^{-1}$ , which can be attributed to the hydrogen bond O-H stretching vibrations and flexural vibration of intra- and intermolecular hydrogen bonds [45,69]. The change in intensity of peaks in this region observed in the spectra of cellulose treated with ionic liquids, compared to the spectra of samples after enzyme hydrolysis, may be connected with a change in the number and strength of hydrogen bonds. The band at 2900  $\text{cm}^{-1}$  attributed to C-H stretching vibrations is observed in the spectra of all cellulose samples, but the samples treated with ionic liquids show higher intensity [23,45]. The band at 1650  $\text{cm}^{-1}$  visible in the spectra of cellulose treated with ionic liquids can be connected with -OH bending of absorbed water [23,45,70]. The intensity of the band at 1650  $\text{cm}^{-1}$  is higher for cellulose samples treated with ionic liquids than for samples treated with the cellulosic enzyme. This is associated with a larger surface area of cellulose particles with smaller dimensions (Figure 3), and thus a greater ability to adsorb moisture. Moreover, significant changes were found within the vibration bands of the amorphous region at 900  $\text{cm}^{-1}$  and crystalline regions at 1405  $\text{cm}^{-1}$ . The changes indicate a decrease in cellulose crystallinity after the applied material treatment. These observations were confirmed by the XRD analysis (Table 1). The peaks at 1170  $\text{cm}^{-1}$  and 900  $\text{cm}^{-1}$  are connected with C-O stretching or O-H bending and the glycosidic C<sub>1</sub>-H deformation mode, respectively [46]. In turn, the bands at 1405  $\text{cm}^{-1}$  and 1115  $\text{cm}^{-1}$  are attributed to the C-H deformation (asymmetric) and O-H association band in cellulose, respectively [71]. Moreover, in the spectra of treated cellulose samples, especially samples hydrolyzed with ionic liquids, peaks ranging from 1100 to 550  $\text{cm}^{-1}$  were observed, indicating twisting, wagging and deformation modes of anhydro-glucopyranose, which are the characteristic pattern of  $\beta$ -glucosidic linkages [23,45].

### 3.2. DLS Analysis

The average particle size (hydrodynamic diameter) of the enzyme-pretreated cellulose and nanocellulose obtained after the two-step production process assessed by dynamic light scattering (DLS) is presented in Figure 3.

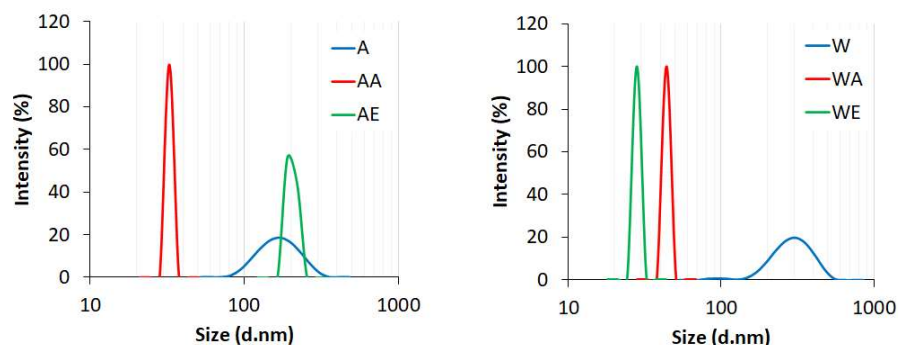


**Figure 3.** The average particle size of (A) enzyme-pretreated Avicel cellulose; (AA) enzyme-pretreated Avicel cellulose treated with AmimCl; (AE) enzyme-pretreated Avicel cellulose treated with EmimOAc; (W) enzyme-pretreated Whatman cellulose; (WA) enzyme-pretreated Whatman cellulose treated with AmimCl; (WE) enzyme-pretreated Whatman cellulose treated with EmimOAc.

The enzymatic hydrolysis of cellulosic materials (Avicel and Whatman) resulted in a decrease of the average particle size, compared to the starting material with a micrometric size. After enzyme-pretreatment the average size of Avicel cellulose particles was below 200 nm, while the particle size of Whatman cellulose was about 300 nm. However, both of the peaks are wide, which indicate high particle size dispersion. According to literature data, the average particle size of cellulose hydrolyzed with the cellulase enzyme was 0.526  $\mu\text{m}$ ; however, 50% of the particles were smaller than this dimension [69]. The average size of cellulose nanocrystals obtained by the endoglucanase enzyme hydrolysis with two heating models (conventional and microwave coupled with ultrasonication) ranged from 100 nm to 3.5  $\mu\text{m}$  [72]. In turn, the particle size of nanocellulose prepared through enzymatic hydrolysis with three different pretreatments (ultrasonic, treatment with NaOH and treatment with DMSO) depended on the pretreatment type. The average size of nanocellulose with ultrasonic pretreatment was 5-6 nm, for that prepared by DMSO-pretreatment it was about 250 nm, while that obtained with NaOH-pretreatment contained two particle types – one of 25 nm and the other of 250 nm, which were the aggregates [70].

The results presented in Figure 3 indicate a notable shift in cellulose particle size after treatment with both ionic liquids (except for Avicel cellulose treated with EmimOAc), as compared to the enzyme-pretreated cellulose. In addition, all nanocellulose samples were characterized by much lower particle size dispersion than samples after enzymatic hydrolysis, which confirmed narrow and well-defined peaks presented at Figure 3. The average particle size of enzyme-pretreated Avicel cellulose after hydrolysis with AmimCl (AA) and enzyme-pretreated Whatman cellulose after hydrolysis with EmimOAc (WE) was around 30 nm, while that of enzyme-pretreated Whatman cellulose after hydrolysis with AmimCl (WA) was around 40 nm. In turn, the nanocellulose obtained by Avicel cellulose hydrolysis with EmimOAc (AE) was characterized by the greater average size of particles (around 200 nm), compared to the other nanocellulose samples after hydrolysis with ionic liquids. To sum up, the results of DLS analysis confirmed that the efficiency of

nanocellulose production with enzyme-pretreatment is influenced by the type of the initial cellulosic material, as well as the type of the used ionic liquid.

### 3.3. SEM Analysis

The morphology of the cellulosic materials after enzymatic pretreatment followed by hydrolysis with ionic liquids was examined by SEM analysis. The SEM images taken are shown in Figure 4.

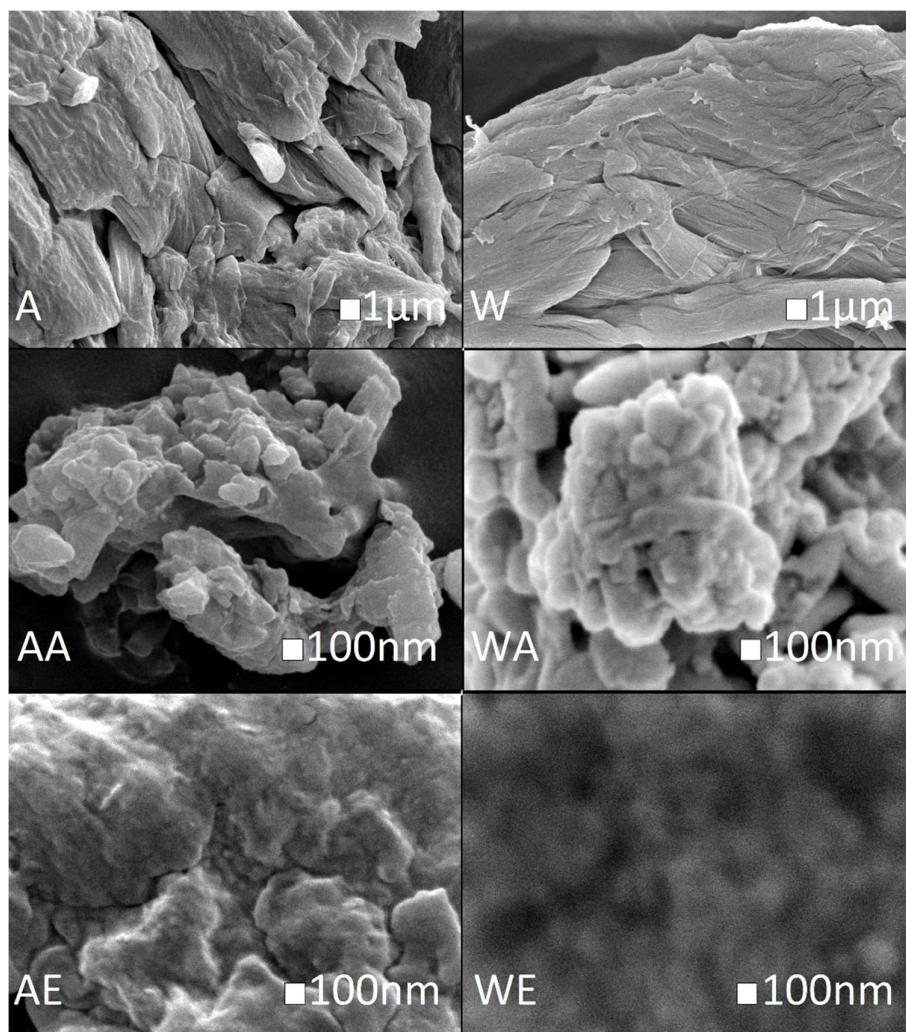


**Figure 4.** SEM images of (A) enzyme-pretreated Avicel cellulose; (AA) enzyme-pretreated Avicel cellulose treated with AmimCl; (AE) enzyme-pretreated Avicel cellulose treated with EmimOAc; (W) enzyme-pretreated Whatman cellulose; (WA) enzyme-pretreated Whatman cellulose treated with AmimCl; (WE) enzyme-pretreated Whatman cellulose treated with EmimOAc.

They displayed that hydrolysis of enzyme-pretreated cellulose (Avicel and Whatman) with both ionic liquids caused changes in the material structure and a reduction of its diameter. The cellulose material after treatment with ionic liquids had a more regular and spherical structure than cellulose hydrolyzed with the *Trichoderma reesei* enzyme. The spherical structure of obtained nanocellulose is in contrast to the results of other research, where nanocellulose produced by hydrolysis with an ionic liquid has a needle or rod-like morphology [23,42,45,73].

### 3.4. XRD Analysis

The diffraction profiles of enzyme-pretreated cellulose and cellulose after treatment with ionic liquids are shown in Figure 5.

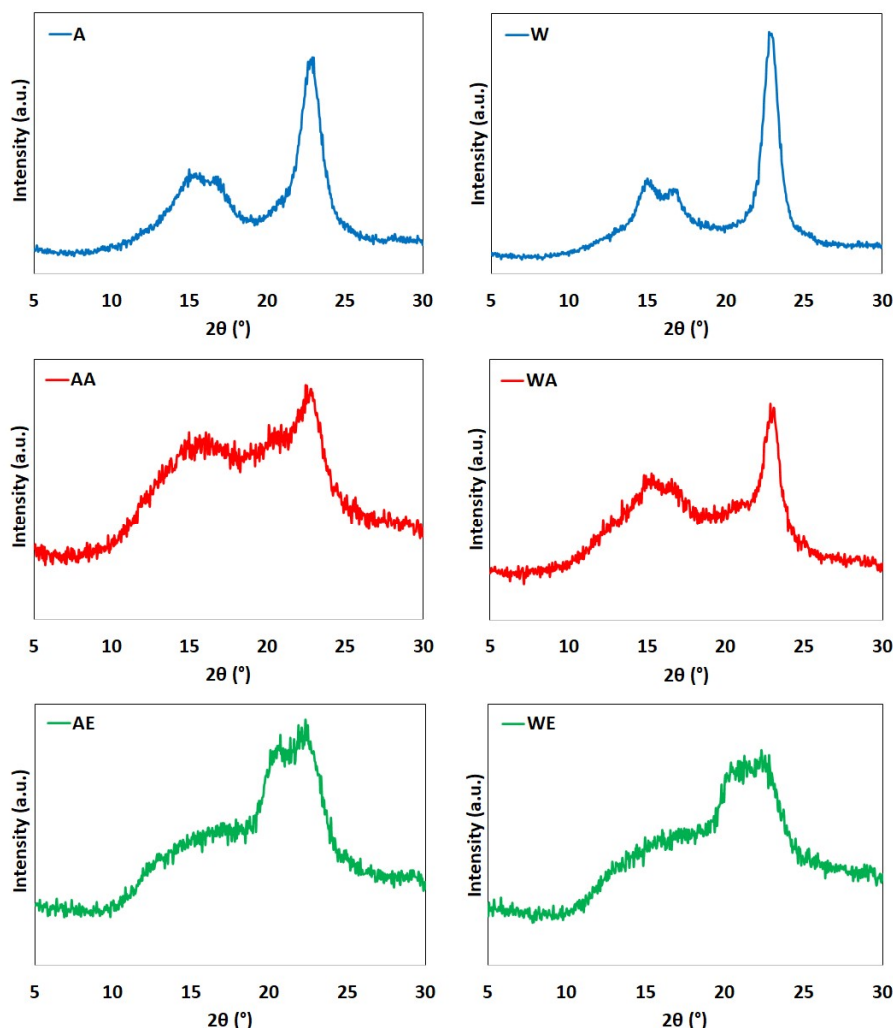


**Figure 5.** XRD patterns of (A) enzyme-pretreated Avicel cellulose; (AA) enzyme-pretreated Avicel cellulose treated with AmimCl; (AE) enzyme-pretreated Avicel cellulose treated with EmimOAc; (W) enzyme-pretreated Whatman cellulose; (WA) enzyme-pretreated Whatman cellulose treated with AmimCl; (WE) enzyme-pretreated Whatman cellulose treated with EmimOAc.

The diffractograms of cellulose after enzymatic hydrolysis (Avicel and Whatman) showed peaks characteristic of cellulose I at  $2\theta = 15^\circ$  (plane 1-10),  $17^\circ$  (plane 110), and  $22.7^\circ$  (plane 200) [74]. Also, these maxima were observed for the enzyme-pretreated cellulose samples treated with AmimCl, although the intensity was much lower.

Unexpectedly, in the case of enzyme-pretreated cellulose treated with EmimOAc, the disappearance of the maximum from cellulose I was found as well as the formation of two maxima at the diffraction angle of  $20^\circ$  and  $22^\circ$ . These peaks came from the lattice planes (110) and (020), respectively. This indicates the formation of cellulose II and proves that the use of the 1-ethyl-3-methylimidazolium acetate solution resulted in the conversion of polymorphic cellulose I into cellulose II. Literature data [75,76] indicated that the conversion of cellulose I into cellulose II was the result of a mercerization process run in the presence of alkali. Also, Cheng et al. [77] noted that the use of 1-ethyl-3-methyl

imidazolium acetate for modification of cellulose, switchgrass (*Panicum virgatum*), pine (*Pinus radiata*), and eucalyptus (*Eucalyptus globulus*) affects the formation of cellulose II. The transformation of cellulose I into cellulose II was also noted by Li et al. [77] and by Wang et al. [78] for another ionic liquid, such as 1-butyl-3-methylimidazolium chloride.

Table 1 presents the crystallinity index of cellulose samples.

**Table 1.** The crystallinity index of cellulose samples.

Samples	The crystallinity index (%)	Samples	The crystallinity index (%)
A	60	W	63
AA	24	WA	33
AE	36	WE	39

The values of the crystallinity index indicate that enzymatic hydrolysis affected the degree of crystallinity of raw cellulose material. The crystallinity index of enzyme-pretreated cellulose was 60% for Avicel and 63% for Whatman, compared to 61% and 75% for untreated raw Avicel and Whatman cellulose, respectively [42,79]. However, significant changes in the degree of crystallinity were noted for the cellulose samples after hydrolysis with ionic liquids. The calculated crystallinity index values of Avicel cellulose after the reaction with ionic liquids were 24% (after hydrolysis with AmimCl) and 36% (after hydrolysis with EmimOAc). The degree of crystallinity for Whatman cellulose after the reaction with ionic liquids was 33% (after hydrolysis with AmimCl) and 39% (after hydrolysis with EmimOAc). Among all the cellulose samples, the nanocellulose sample with the smallest particle size (AA) (Figure 3) was characterized by the lowest crystallinity. This indicates that the cellulose chains were broken during the treatment process with ionic liquids, with a consequent reduction in the degree of crystallinity. The reaction of enzyme-pretreated cellulose with AmimCl caused a decrease of crystallinity index by about 60% for Avicel cellulose and 48% for Whatman cellulose compared to the enzyme-pretreated material. The reduction in the degree of crystallinity for cellulose treated with ionic liquids was previously reported by other authors [42,73,80]. The degree of crystallinity of eucalyptus pulp amounting to 70% was reduced to 36% by treatment with an ionic liquid – BmimCl [80]. The degree of crystallinity for nanocellulose obtained from cotton and microcrystalline cellulose treated with BmimCl was 52% and 62%, compared to the values of 77% and 80% for the native material, respectively [48]. The degree of crystallinity of nanocellulose obtained with EmimOAc (33%) was lower than the degree of crystallinity of nanocellulose obtained in our previous work, where EmimCl (47%) was used [42]. According to the literature data, the anion of the ionic liquid plays an important role in the hydrolysis process of cellulose, which forms hydrogen bonds with -OH groups of cellulose. The research indicated that the acetate anion forms strong hydrogen bonds, as opposed to the weakly basic chloride anion which forms weak hydrogen bonds with cellulose [24,51].

### 3.5. TG Analysis

The thermogravimetric curve (TG) and its derivative curve (DTG) of enzyme-pretreated cellulose (in the form of Avicel and Whatman) hydrolyzed with ionic liquids are showed in Figure 6 and Figure 7, respectively.

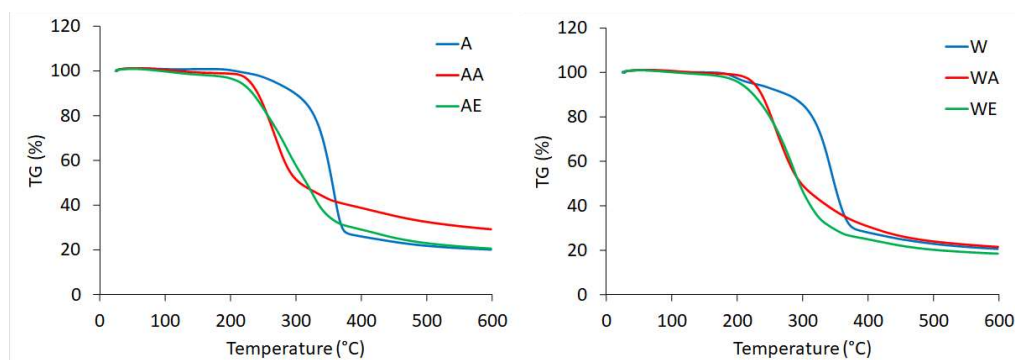


**Figure 6.** TG curves of (A) enzyme-pretreated Avicel cellulose; (AA) enzyme-pretreated Avicel cellulose treated with AmimCl; (AE) enzyme-pretreated Avicel cellulose treated with EmimOAc; (W) enzyme-pretreated Whatman cellulose; (WA) enzyme-pretreated Whatman cellulose treated with AmimCl; (WE) enzyme-pretreated Whatman cellulose treated with EmimOAc.

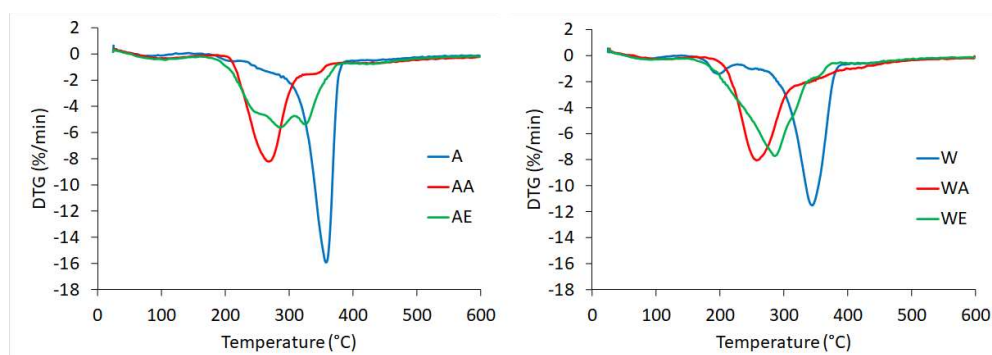


**Figure 7.** DTG curves of (A) enzyme-pretreated Avicel cellulose; (AA) enzyme-pretreated Avicel cellulose treated with AmimCl; (AE) enzyme-pretreated Avicel cellulose treated with EmimOAc; (W) enzyme-pretreated Whatman cellulose; (WA) enzyme-pretreated Whatman cellulose treated with AmimCl; (WE) enzyme-pretreated Whatman cellulose treated with EmimOAc.

Knowledge of the thermostability of nanocellulose is important e.g. when this material is used as a filler for a biopolymer, where elevated temperatures are required for their production [27,62,81]. Raw cellulose is a material with moderate thermal properties, with the decomposition temperature between 315 – 400 °C [82]. The TG and DTG curves for enzyme hydrolyzed cellulose differed from those for enzyme-pretreated cellulose after the reaction with both ionic liquids, which indicated that hydrolysis with ionic liquids results in changes in the characteristic degradation temperatures. All the tested samples initially showed a slight loss of weight at temperatures below 100 °C, which is related to water evaporation [45]. The presence of hydrogen bonds in the tested cellulose material was confirmed by FTIR analysis (Figure 1). In the curves of all the samples, except for the EmimOAc treated cellulose, a single significant decomposition was observed corresponding to the degradation processes such as dehydration, depolymerization and degradation of the glycosyl rings followed by the formation of a charred residue [69]. The DTG curve for the enzyme-pretreated Avicel cellulose hydrolyzed with EmimOAc showed a different course of its thermal decomposition (two peaks on the DTG curve) and thermal characteristics (thermal properties) compared to the other cellulose samples. The thermal behavior of this cellulose sample can be explained by the particle size (around 200 nm), which is greater than that of the other nanocellulose samples. This may cause thermal degradation to take place in multiple stages (two peaks) and be slower (the maximum rates of decomposition are lower compared to the other tested samples - the y axis [% / min] on the DTG curves). The onset temperature of degradation ( $T_{\text{onset}}$ ) and the maximum

decomposition temperature ( $T_{\max}$ ) of the enzyme-pretreated Avicel cellulose were 300 and 358 °C, respectively. In turn, decomposition of the enzyme-pretreated Whatman cellulose took place within a range of temperatures of 293 – 379 °C.

Degradation behavior of the enzyme-pretreated cellulose hydrolyzed with ionic liquids presents differences from that of the cellulose treated only with the enzyme, implying that the degradation started at lower temperatures 211 °C (Avicel) and 188 °C (Whatman) for cellulose treated with AmimCl and 194 °C (Avicel) and 200 °C (Whatman) for cellulose treated with EmimOAc. The beginning of decomposition for the enzyme-pretreated cellulose after the reaction with ionic liquids at a lower temperatures is connected with a lower crystallinity index of cellulose treated with AmimCl and EmimOAc. The high surface area of cellulose nanoparticles also reduces their thermal properties, because of the greater surface area exposed to high temperature [69]. The nanocellulose obtained by different methods was characterized by various thermal stability. The onset temperatures of enzyme-pretreated cellulose after the reaction with both ionic liquids are lower than that for nanocellulose from wood (280 °C), maize husk (291 °C) and sugar cane (319 °C) described in a paper by Onkarappa et al. [71]. In turn, decomposition of cellulose nanocrystals obtained by hydrolysis with sulfuric acid started at around 150 °C, as described by Lu and Hsieh [83]. The nanocellulose obtained by hydrolysis with BmimCl showed lower thermal stability with the decomposition temperature of 238 °C, compared to 288 °C determined for raw cellulose [84]. Lower thermal stability was also exhibited by nanocellulose produced by hydrolysis with BmimHSO<sub>4</sub>, compared to native microcrystalline cellulose [45].

#### 4. Conclusions

The present work has demonstrated that nanocellulose could be produced through hydrolysis with ionic liquids from enzyme-pretreated microcrystalline cellulose. In this study, ionic liquids (1-ethyl-3-methylimidazole acetate (EmimOAc) and 1-allyl-3-methylimidazolium chloride (AmimCl)) were used. The ionic liquid treatment of the cellulosic material (Avicel and Whatman) resulted in a decrease of the average particle size, compared to the material after enzymatic hydrolysis. The nanocellulose samples were found to have a regular and spherical structure with a diameter of about 30-40 nm. The exception was cellulose obtained from the enzyme-pretreated Avicel cellulose by hydrolysis with EmimOAc, which had a particle size of about 200 nm. The basic cellulose I structure was preserved in cellulose after hydrolysis with the *Trichoderma reesei* enzyme and nanocellulose obtained through AmimCl treatment. In the case of enzyme-pretreated cellulose treated with EmimOAc the transformation to cellulose II occurred. All nanocellulose samples showed a decrease in the crystallinity index compared to the material after enzymatic hydrolysis. Moreover, treatment with ionic liquids changed thermal properties of nanocellulose, resulting in a decrease in their thermal stability.

Overall, the two-step process involving enzyme-pretreatment and hydrolysis with ionic liquids resulted in the production of nanocellulose. The presented results indicated that the particle size of nanocellulose and its structure depend on the ionic liquid used.

**Author Contributions:** Conceptualization, M.B.; methodology, M.B.; formal analysis, M.B., K.S., M.B., B.P., K.D., S.B.; writing – original draft preparation, M.B.; writing – review and editing, M.W.; supervision, I.R. All the authors have read and agreed to the published version of the manuscript.

**Funding:** The paper was co-financed within the framework of the Ministry of Science and Higher Education program 'Regional Initiative of Excellence' in the years 2019–2022, Project No. 005/RID/2018/19. This work was supported by the National Science Centre, Poland (Grant number 2014/13/B/NZ9/02442) and was funded in part by the Ministry of Education and Science.

**Institutional Review Board Statement:** Not applicable.

**Informed Consent Statement:** Not applicable.

**Data Availability Statement:** The data reported in this study are available from the authors upon request.

**Conflicts of Interest:** The authors declare no conflict of interest.

## References

- Ribeiro, R.S.A.; Pohlmann, B.C.; Calado, V.; Bojorge, N.; Pereira, N. Production of nanocellulose by enzymatic hydrolysis: Trends and challenges. *Eng. Life Sci.* **2019**, *19*, 279–291, doi:10.1002/elsc.201800158.
- Charreau, H.; Cavallo, E.; Foresti, M.L. Patents involving nanocellulose: Analysis of their evolution since 2010. *Carbohydr. Polym.* **2020**, *237*, 116039, doi:10.1016/j.carbpol.2020.116039.
- Ahankari, S.S.; Subhedar, A.R.; Bhadauria, S.S.; Dufresne, A. Nanocellulose in food packaging: A review. *Carbohydr. Polym.* **2021**, *255*, 117479, doi:10.1016/j.carbpol.2020.117479.
- Zinge, C.; Kandasubramanian, B. Nanocellulose based biodegradable polymers. *Eur. Polym. J.* **2020**, *133*, 109758, doi:10.1016/j.eurpolymj.2020.109758.
- Moohan, J.; Stewart, S.A.; Espinosa, E.; Rosal, A.; Rodríguez, A.; Larrañeta, E.; Donnelly, R.F.; Domínguez-Robles, J. Cellulose nanofibers and other biopolymers for biomedical applications. A review. *Appl. Sci.* **2020**, *10*, doi:10.3390/app10010065.
- Karimian, A.; Parsian, H.; Majidinia, M.; Rahimi, M.; Mir, S.M.; Samadi Kafil, H.; Shafiei-Irannejad, V.; Kheyrollah, M.; Ostadi, H.; Yousefi, B. Nanocrystalline cellulose: Preparation, physicochemical properties, and applications in drug delivery systems. *Int. J. Biol. Macromol.* **2019**, *133*, 850–859, doi:10.1016/j.ijbiomac.2019.04.117.
- Bacakova, L.; Pajorova, J.; Bacakova, M.; Skogberg, A.; Kallio, P.; Kolarova, K.; Svoricik, V. Versatile application of nanocellulose: From industry to skin tissue engineering and wound healing. *Nanomaterials* **2019**, *9*, doi:10.3390/nano9020164.
- Trache, D.; Tarchoun, A.F.; Derradji, M.; Hamidon, T.S.; Masruchin, N.; Brosse, N.; Hussin, M.H. *Nanocellulose: From Fundamentals to Advanced Applications*; 2020; Vol. 8; ISBN 0000000230049.
- Abdul Khalil, H.P.S.; Jummaat, F.; Yahya, E.B.; Olaiya, N.G.; Adnan, A.S.; Abdat, M.; Nasir, N.A.M.; Halim, A.S.; Seeta Uthaya Kumar, U.; Bairwan, R.; et al. A review on micro- to nanocellulose biopolymer scaffold forming for tissue engineering applications. *Polymers* **2020**, *12*, 1–36, doi:10.3390/POLYM12092043.
- Lengowski, E.C.; Bonfatti Júnior, E.A.; Nishidate Kumode, M.M.; Carneiro, M.E.; Satyanarayana, K.G. Nanocellulose-reinforced adhesives for wood-based panels. *Sustain. Polym. Compos. Nanocomposites* **2019**, 1001–1025, doi:10.1007/978-3-030-05399-4\_35.
- Nemoto, J.; Saito, T.; Isogai, A. Simple freeze-drying procedure for producing nanocellulose aerogel-containing, high-performance air filters. *ACS Appl. Mater. Interfaces* **2015**, *7*, 19809–19815, doi:10.1021/acsami.5b05841.
- Putro, J.N.; Kurniawan, A.; Ismadji, S.; Ju, Y.H. Nanocellulose based biosorbents for wastewater treatment: Study of isotherm, kinetic, thermodynamic and reusability. *Environ. Nanotechnology, Monit. Manag.* **2017**, *8*, 134–149, doi:10.1016/j.enmm.2017.07.002.
- Zhou, Y.; Khan, T.M.; Liu, J.C.; Fuentes-Hernandez, C.; Shim, J.W.; Najafabadi, E.; Youngblood, J.P.; Moon, R.J.; Kippelen, B. Efficient recyclable organic solar cells on cellulose nanocrystal substrates with a conducting polymer top electrode deposited by film-transfer lamination. *Org. Electron.* **2014**, *15*, 661–666, doi:10.1016/j.orgel.2013.12.018.
- Mohammed, N.; Grishkewich, N.; Berry, R.M.; Tam, K.C. Cellulose nanocrystal–alginate hydrogel beads as novel adsorbents for organic dyes in aqueous solutions. *Cellulose* **2015**, *22*, 3725–3738, doi:10.1007/s10570-015-0747-3.
- Lasrado, D.; Ahankari, S.; Kar, K. Nanocellulose-based polymer composites for energy applications—A review. *J. Appl. Polym. Sci.* **2020**, *137*, 1–14, doi:10.1002/app.48959.
- Phanthong, P.; Reubroycharoen, P.; Hao, X.; Xu, G.; Abudula, A.; Guan, G. Nanocellulose: Extraction and application. *Carbon Resour. Convers.* **2018**, *1*, 32–43, doi:10.1016/j.crcon.2018.05.004.

17. Abitbol, T.; Rivkin, A.; Cao, Y.; Nevo, Y.; Abraham, E.; Ben-Shalom, T.; Lapidot, S.; Shoseyov, O. Nanocellulose, a tiny fiber with huge applications. *Curr. Opin. Biotechnol.* **2016**, *39*, 76–88, doi:10.1016/j.copbio.2016.01.002.
18. Heise, K.; Kontturi, E.; Allahverdiyeva, Y.; Tammelin, T.; Linder, M.B.; Nonappa; Ikkala, O. Nanocellulose: Recent fundamental advances and emerging biological and biomimicking applications. *Adv. Mater.* **2021**, *33*, doi:10.1002/adma.202004349.
19. George, J.; Sabapathi, S.N. Cellulose nanocrystals: Synthesis, functional properties, and applications. *Nanotechnol. Sci. Appl.* **2015**, *8*, 45–54, doi:10.2147/NSA.S64386.
20. Kalia, S.; Dufresne, A.; Cherian, B.M.; Kaith, B.S.; Avérous, L.; Njuguna, J.; Nassiopoulos, E. Cellulose-based bio- and nanocomposites: A review. *Int. J. Polym. Sci.* **2011**, *2011*, doi:10.1155/2011/837875.
21. Lee, H. V.; Hamid, S.B.A.; Zain, S.K. Conversion of lignocellulosic biomass to nanocellulose: Structure and chemical process. *Sci. World J.* **2014**, *2014*, doi:10.1155/2014/631013.
22. De Aguiar, J.; Bondancia, T.J.; Claro, P.I.C.; Mattoso, L.H.C.; Farinas, C.S.; Marconcini, J.M. Enzymatic Deconstruction of sugarcane bagasse and straw to obtain cellulose nanomaterials. *ACS Sustain. Chem. Eng.* **2020**, *8*, 2287–2299, doi:10.1021/acssuschemeng.9b06806.
23. Man, Z.; Muhammad, N.; Sarwono, A.; Bustam, M.A.; Kumar, M.V.; Rafiq, S. Preparation of cellulose nanocrystals using an ionic liquid. *J. Polym. Environ.* **2011**, *19*, 726–731, doi:10.1007/s10924-011-0323-3.
24. Du, H.; Qian, X. The effects of acetate anion on cellulose dissolution and reaction in imidazolium ionic liquids. *Carbohydr. Res.* **2011**, *346*, 1985–1990, doi:10.1016/j.carres.2011.05.022.
25. Clough, M.T.; Geyey K.; Hunt P.A.; Son S.; Vagt U.; Welton T. Ionic liquids: not always innocent solvents for cellulose. *Green Chem.* **2014**, *00*, 1-15, doi: 10.1039/C4GC01955E.
26. Handy, S.T.; Okello, M. The 2-position of imidazolium ionic liquids: Substitution and exchange. *J. Org. Chem.* **2005**, *70*, 1915–1918, doi:10.1021/jo0480850.
27. Michelin, M.; Gomes, D.G.; Romaní, A.; Polizeli, M. de L.T.M.; Teixeira, J.A. Nanocellulose production: Exploring the enzymatic route and residues of pulp and paper industry. *Molecules* **2020**, *25*, 1–36, doi:10.3390/molecules25153411.
28. Zielińska, D.; Szentner, K.; Waśkiewicz, A.; Sławomir, B. Production of nanocellulose by enzymatic treatment for application in polymer composites. *Materials* **2021**, *1*–26, doi: 10.3390/ma14092124.
29. Mussatto, S.; Teixeira, J. Lignocellulose as raw material in fermentation processes. *Current Research, Technology and Education Topics in Applied Microbiology and Microbial Biotechnology*; 2010; vol. 2; 897-907; ISBN-13: 978-84-614-6195-0.
30. Josefsson, P.; Henriksson, G.; Wågberg, L. The physical action of cellulases revealed by a quartz crystal microbalance study using ultrathin cellulose films and pure cellulases. *Biomacromolecules* **2008**, *9*, 249–254, doi:10.1021/bm700980b.
31. Cui, S.; Zhang, S.; Ge, S.; Xiong, L.; Sun, Q. Green preparation and characterization of size-controlled nanocrystalline cellulose via ultrasonic-assisted enzymatic hydrolysis. *Ind. Crops Prod.* **2016**, *83*, 346–352, doi:10.1016/j.indcrop.2016.01.019.
32. Siqueira, G.A.; Dias, I.K.R.; Arantes, V. Exploring the action of endoglucanases on bleached eucalyptus kraft pulp as potential catalyst for isolation of cellulose nanocrystals. *Int. J. Biol. Macromol.* **2019**, *133*, 1249–1259, doi:10.1016/j.ijbiomac.2019.04.162.
33. Tibolla, H.; Pelissari, F.M.; Martins, J.T.; Lanzoni, E.M.; Vicente, A.A.; Menegalli, F.C.; Cunha, R.L. Banana starch nanocomposite with cellulose nanofibers isolated from banana peel by enzymatic treatment: In vitro cytotoxicity assessment. *Carbohydr. Polym.* **2019**, *207*, 169–179, doi:10.1016/j.carbpol.2018.11.079.
34. Yassin, M.A.; Gad, A.A.M.; Ghanem, A.F.; Abdel Rehim, M.H. Green synthesis of cellulose nanofibers using immobilized cellulase. *Carbohydr. Polym.* **2019**, *205*, 255–260, doi:10.1016/j.carbpol.2018.10.040.
35. Pääkko, M.; Ankerfors, M.; Kosonen, H.; Nykänen, A.; Ahola, S.; Österberg, M.; Ruokolainen, J.; Laine, J.; Larsson, P.T.; Ikkala, O.; et al. Enzymatic hydrolysis combined with mechanical shearing and high-pressure homogenization for nanoscale cellulose fibrils and strong gels. *Biomacromolecules* **2007**, *8*, 1934–1941, doi:10.1021/bm061215p.

36. Dai, J.; Chae, M.; Beyene, D.; Danumah, C.; Tosto, F.; Bressler, D.C. Co-production of cellulose nanocrystals and fermentable sugars assisted by endoglucanase treatment of wood pulp. *Materials*. **2018**, *11*, doi:10.3390/ma11091645.
37. Camargo, L.A.; Pereira, S.C.; Correa, A.C.; Farinas, C.S.; Marconcini, J.M.; Mattoso, L.H.C. Feasibility of Manufacturing cellulose nanocrystals from the solid residues of second-generation ethanol production from *Sugarcane Bagasse*. *Bioenergy Res.* **2016**, *9*, 894–906, doi:10.1007/s12155-016-9744-0.
38. Beltramino, F.; Blanca Roncero, M.; Vidal, T.; Valls, C. A novel enzymatic approach to nanocrystalline cellulose preparation. *Carbohydr. Polym.* **2018**, *189*, 39–47, doi:10.1016/j.carbpol.2018.02.015.
39. Grzabka-Zasadzińska, A.; Smutek, W.; Kaczorek, E.; Borysiak, S. Chitosan biocomposites with enzymatically produced nanocrystalline cellulose. *Polym. Compos.* **2017**, *16*, 101–113, doi: 10.1002/pc.24552.
40. Phanthong, P.; Karnjanakom, S.; Reubroycharoen, P.; Hao, X.; Abudula, A.; Guan, G. A facile one-step way for extraction of nanocellulose with high yield by ball milling with ionic liquid. *Cellulose* **2017**, *24*, 2083–2093, doi:10.1007/s10570-017-1238-5.
41. Pacheco, C.M.; Bustos, A. C.; Reyes, G. Cellulose nanocrystals from blueberry pruning residues isolated by ionic liquids and TEMPO-oxidation combined with mechanical disintegration. *J. Dispers. Sci. Technol.* **2020**, *41*, 1731–1741, doi:10.1080/01932691.2020.1775092.
42. Babicka, M.; Woźniak, M.; Dwiecki, K.; Borysiak, S.; Ratajczak, I. Preparation of nanocellulose using ionic liquids: 1-propyl-3-methylimidazolium chloride and 1-ethyl-3-methylimidazolium chloride. *Molecules* **2020**, *25*, 1–13, doi:10.3390/molecules25071544.
43. Jordan, J.H.; Easson, M.W.; Condon, B.D. Cellulose hydrolysis using ionic liquids and inorganic acids under dilute conditions: Morphological comparison of nanocellulose. *RSC Adv.* **2020**, *10*, 39413–39424, doi:10.1039/d0ra05976e.
44. Prudêncio, C.; Vieira, M.; Van der Auweraer, S.; Ferraz, R. Recycling old antibiotics with ionic liquids. *Antibiotics* **2020**, *9*, 1–16, doi:10.3390/antibiotics9090578.
45. Tan, X.Y.; Abd Hamid, S.B.; Lai, C.W. Preparation of high crystallinity cellulose nanocrystals (CNCs) by ionic liquid solvolysis. *Biomass and Bioenergy* **2015**, *81*, 584–591, doi:10.1016/j.biombioe.2015.08.016.
46. Mao, J.; Abushammala, H.; Hettegger, H.; Rosenau, T.; Laborie, M.P. Imidazole, a new tunable reagent for producing nanocellulose, part I: Xylan-coated CNCs and CNFs. *Polymers* **2017**, *9*, 1–11, doi:10.3390/polym9100473.
47. Mao, J.; Abushammala, H.; Pereira, L.B.; Laborie, M.P. Swelling and hydrolysis kinetics of Kraft pulp fibers in aqueous 1-butyl-3-methylimidazolium hydrogen sulfate solutions. *Carbohydr. Polym.* **2016**, *153*, 284–291, doi:10.1016/j.carbpol.2016.07.092.
48. Han, J.; Zhou, C.; French, A.D.; Han, G.; Wu, Q. Characterization of cellulose II nanoparticles regenerated from 1-butyl-3-methylimidazolium chloride. *Carbohydr. Polym.* **2013**, *94*, 773–781, doi:10.1016/j.carbpol.2013.02.003.
49. Mao, J.; Osorio-Madrado, A.; Laborie, M.P. Preparation of cellulose I nanowhiskers with a mildly acidic aqueous ionic liquid: Reaction efficiency and whiskers attributes. *Cellulose* **2013**, *20*, 1829–1840, doi:10.1007/s10570-013-9942-2.
50. Abushammala, H.; Krossing, I.; Laborie, M.P. Ionic liquid-mediated technology to produce cellulose nanocrystals directly from wood. *Carbohydr. Polym.* **2015**, *134*, 609–616, doi:10.1016/j.carbpol.2015.07.079.
51. Grzabka-Zasadzińska, A.; Skrzypczak, A.; Borysiak, S. The influence of the cation type of ionic liquid on the production of nanocrystalline cellulose and mechanical properties of chitosan-based biocomposites. *Cellulose* **2019**, *26*, 4827–4840, doi:10.1007/s10570-019-02412-1.
52. Brandt, A.; Gräsvik, J.; Hallett, J.P.; Welton, T. Deconstruction of lignocellulosic biomass with ionic liquids. *Green Chem.* **2013**, *15*, 550–583, doi:10.1039/c2gc36364j.
53. Suhas, D.; Gupta, V.K.; Carrott, P.J.M.; Singh, R.; Chaudhary, M.; Kushwaha, S. Cellulose: A review as natural, modified and activated carbon adsorbent. *Bioresour. Technol.* **2016**, *216*, 1066–1076, doi:10.1016/j.biortech.2016.05.106.
54. Moon, R.J.; Martini, A.; Nairn, J.; Simonsen, J.; Youngblood, J. *Cellulose nanomaterials review: Structure, properties and*

- nanocomposites*; 2011; Vol. 40; ISBN 1765496829.
55. Noor, S.M.; Anuar, A.N.; Tamunaidu, P.; Goto, M.; Shameli, K.; Halim, M.H.A. Nanocellulose production from natural and recyclable sources: A review. *IOP Conf. Ser. Earth Environ. Sci.* **2020**, *479*, doi:10.1088/1755-1315/479/1/012027.
  56. Brodeur, G.; Yau, E.; Badal, K.; Collier, J.; Ramachandran, K.B.; Ramakrishnan, S. Chemical and physicochemical pretreatment of lignocellulosic biomass: A review. *Enzyme Res.* **2011**, *2011*, doi:10.4061/2011/787532.
  57. Siró, I.; Plackett, D. Microfibrillated cellulose and new nanocomposite materials: A review. *Cellulose* **2010**, *17*, 459–494, doi:10.1007/s10570-010-9405-y.
  58. Bensah, E.C.; Mensah, M. Chemical pretreatment methods for the production of cellulosic ethanol: Technologies and innovations. *Int. J. Chem. Eng.* **2013**, *2013*, doi:10.1155/2013/719607.
  59. Bali, G.; Meng, X.; Deneff, J.I.; Sun, Q.; Ragauskas, A.J. The effect of alkaline pretreatment methods on cellulose structure and accessibility. *ChemSusChem* **2015**, *8*, 275–279, doi:10.1002/cssc.201402752.
  60. Pirich, C.L.; Picheth, G.F.; Fontes, A.M.; Delgado-Aguilar, M.; Ramos, L.P. Disruptive enzyme-based strategies to isolate nanocelluloses: a review. *Cellulose* **2020**, *27*, 5457–5475, doi:10.1007/s10570-020-03185-8.
  61. Chen, X.Q.; Pang, G.X.; Shen, W.H.; Tong, X.; Jia, M.Y. Preparation and characterization of the ribbon-like cellulose nanocrystals by the cellulase enzymolysis of cotton pulp fibers. *Carbohydr. Polym.* **2019**, *207*, 713–719, doi:10.1016/j.carbpol.2018.12.042.
  62. Squinca, P.; Bilatto, S.; Badino, A.C.; Farinas, C.S. Nanocellulose production in future biorefineries: An integrated approach using tailor-made enzymes. *ACS Sustain. Chem. Eng.* **2020**, *8*, 2277–2286, doi:10.1021/acssuschemeng.9b06790.
  63. Ming-Ju Chen, Kreuter, J.Y.-T.K. Nanoparticles and microparticles for drug and vaccine delivery. *J. Anat.* **1996**, *189* ( Pt 3, 503–505, doi:10.1002/bit.
  64. Li, C.; Knierim, B.; Manisseri, C.; Arora, R.; Scheller, H. V.; Auer, M.; Vogel, K.P.; Simmons, B.A.; Singh, S. Comparison of dilute acid and ionic liquid pretreatment of switchgrass: Biomass recalcitrance, delignification and enzymatic saccharification. *Bioresour. Technol.* **2010**, *101*, 4900–4906, doi:10.1016/j.biortech.2009.10.066.
  65. Zhao, H.; Jones, C.L.; Baker, G.A.; Xia, S.; Olubajo, O.; Person, V.N. Regenerating cellulose from ionic liquids for an accelerated enzymatic hydrolysis. *J. Biotechnol.* **2009**, *139*, 47–54, doi:10.1016/j.jbiotec.2008.08.009.
  66. Lee, S.H.; Doherty, T. V.; Linhardt, R.J.; Dordick, J.S. Ionic liquid-mediated selective extraction of lignin from wood leading to enhanced enzymatic cellulose hydrolysis. *Biotechnol. Bioeng.* **2009**, *102*, 1368–1376, doi:10.1002/bit.22179.
  67. Hindeleh, A.M.; Johnson, D.J. The resolution of multipeak data in fibre science. *J. Phys. D. Appl. Phys.* **1971**, *4*, 259–263, doi:10.1088/0022-3727/4/2/311.
  68. Rabiej, S. A comparison of two X-ray diffraction procedures for crystallinity determination. *Eur. Polym. J.* **1991**, *27*, 947–954, doi:10.1016/0014-3057(91)90038-P.
  69. Fattahi Meyabadi, T.; Dadashian, F.; Mir Mohamad Sadeghi, G.; Ebrahimi Zanjani Asl, H. Spherical cellulose nanoparticles preparation from waste cotton using a green method. *Powder Technol.* **2014**, *261*, 232–240, doi:10.1016/j.powtec.2014.04.039.
  70. Chen, X.; Deng, X.; Shen, W.; Jiang, L. Controlled enzymolysis preparation of nanocrystalline cellulose from pretreated cotton fibers. *BioResources* **2012**, *7*, 4237–4248, doi:10.15376/biores.7.3.4237-4248.
  71. Onkarappa, H.S.; Prakash, G.K.; Pujar, G.H.; Rajith Kumar, C.R.; Radha; Latha, M.S.; Betageri, V.S. Synthesis and characterization of nanocellulose using renewable resources through Ionic liquid medium. *Adv. Nat. Sci. Nanosci. Nanotechnol.* **2020**, *11*, doi:10.1088/2043-6254/ab9d23.
  72. Filson, P.B.; Dawson-Andoh, B.E.; Schwegler-Berry, D. Enzymatic-mediated production of cellulose nanocrystals from recycled pulp. *Green Chem.* **2009**, *11*, 1808–1814, doi:10.1039/b915746h.
  73. Lazko, J.; Sénéchal, T.; Bouchut, A.; Paint, Y.; Dangreau, L.; Fradet, A.; Tessier, M.; Raquez, J.M.; Dubois, P. Acid-free extraction of cellulose type I nanocrystals using Brønsted acid-type ionic liquids. *Nanocomposites* **2016**, *2*, 65–75,

- doi:10.1080/20550324.2016.1199410.
74. French, A.D. Idealized powder diffraction patterns for cellulose polymorphs. *Cellulose* **2014**, *21*, 885–896, doi:10.1007/s10570-013-0030-4.
  75. Borysiak, S. Influence of cellulose polymorphs on the polypropylene crystallization. *J. Therm. Anal. Calorim.* **2013**, *113*, 281–289, doi:10.1007/s10973-013-3109-0.
  76. Borysiak, S. Influence of wood mercerization on the crystallization of polypropylene in wood/PP composites. *J. Therm. Anal. Calorim.* **2012**; Vol. 109, pp. 595–603.
  77. Cheng, G.; Varanasi, P.; Li, C.; Liu, H.; Melnichenko, Y.B.; Simmons, B.A.; Kent, M.S.; Singh, S. Transition of cellulose crystalline structure and surface morphology of biomass as a function of ionic liquid pretreatment and its relation to enzymatic hydrolysis. *Biomacromolecules* **2011**, *12*, 933–941, doi:10.1021/bm101240z.
  78. Wang, Y.; Wei, X.; Li, J.; Wang, F.; Wang, Q.; Zhang, Y.; Kong, L. Homogeneous isolation of nanocellulose from eucalyptus pulp by high pressure homogenization. *Ind. Crops Prod.* **2017**, *104*, 237–241, doi:10.1016/j.indcrop.2017.04.032.
  79. Costa, M.N.; Veigas, B.; Jacob, J.M.; Santos, D.S.; Gomes, J.; Baptista, P. V.; Martins, R.; Inácio, J.; Fortunato, E. A low cost, safe, disposable, rapid and self-sustainable paper-based platform for diagnostic testing: Lab-on-paper. *Nanotechnology* **2014**, *25*, doi:10.1088/0957-4484/25/9/094006.
  80. Wang, Y.; Wei, X.; Li, J.; Wang, F.; Wang, Q.; Zhang, Y.; Kong, L. Homogeneous isolation of nanocellulose from eucalyptus pulp by high pressure homogenization. *Ind. Crops Prod.* **2017**, *104*, 237–241, doi:10.1016/j.indcrop.2017.04.032.
  81. Miao, J.; Yu, Y.; Jiang, Z.; Zhang, L. One-pot preparation of hydrophobic cellulose nanocrystals in an ionic liquid. *Cellulose* **2016**, *23*, 1209–1219, doi:10.1007/s10570-016-0864-7.
  82. Yang, H.; Yan, R.; Chen, H.; Lee, D.H.; Zheng, C. Characteristics of hemicellulose, cellulose and lignin pyrolysis. *Fuel* **2007**, *86*, 1781–1788, doi:10.1016/j.fuel.2006.12.013.
  83. Lu, P.; Hsieh, Y. Lo Preparation and properties of cellulose nanocrystals: Rods, spheres, and network. *Carbohydr. Polym.* **2010**, *82*, 329–336, doi:10.1016/j.carbpol.2010.04.073.
  84. Li, J.; Wei, X.; Wang, Q.; Chen, J.; Chang, G.; Kong, L.; Su, J.; Liu, Y. Homogeneous isolation of nanocellulose from sugarcane bagasse by high pressure homogenization. *Carbohydr. Polym.* **2012**, *90*, 1609–1613, doi:10.1016/j.carbpol.2012.07.038.